^{1}H-NMR Investigation of the Oxygenation of Hemoglobin in Intact Human Red Blood Cells

Bayard K. Fetler,*‡ Virgil Simplaceanu,* and Chien Ho*
Departments of *Biological Sciences and ‡Physics, Carnegie Mellon University, Pittsburgh, Pennsylvania 15213 USA

ABSTRACT Using improved selective excitation methods for proton nuclear magnetic resonance (NMR), we have conducted measurements of the oxygenation of hemoglobin inside intact human red blood cells. The selective excitation methods use pulse shape-insensitive suppression of the water signal, while producing uniform phase excitation in the region of interest and, thus, are suitable for a wide variety of applications in vivo. We have measured the areas of ^{1}H-NMR resonances of the hyperfine-shifted, exchangeable $N_\delta H$ protons of the proximal histidine residues of the α- and β-chains in deoxyhemoglobin (63 and 76 ppm downfield from the proton resonance of 2,2-dimethyl-2-silapentane-5-sulfonate (DSS), respectively), which are sensitive to the paramagnetic state of the iron, and for which the α- and β-chain resonances are resolved, and from the ring current-shifted γ_2-CH_3 protons of the distal valine residues in oxyhemoglobin (2.4 ppm upfield from DSS), which are sensitive to the conformation of the heme pocket in the oxy state. We have found that the proximal histidine resonances are directly correlated with the degree of oxygenation of hemoglobin, whereas the distal valine resonances appear to be correlated with the conformation in the heme pocket that occurs after the binding of oxygen, in both the presence and absence of 2,3-diphosphoglycerate. In addition, from the proximal histidine resonances, we have observed a preference for the binding of oxygen to the α-chain (up to about 10%) of hemoglobin over the β-chain in both the presence and absence of 2,3-diphosphoglycerate. These new results obtained in intact erythrocytes are consistent with our previous ^{1}H-NMR studies on purified human normal adult hemoglobin. A unique feature of our ^{1}H-NMR method is the ability to monitor the binding of oxygen specifically to the α- and β-chains of hemoglobin both in solution and in intact red blood cells. This information is essential to our understanding of the molecular basis for the hemoglobin molecule serving as the oxygen carrier in vertebrates.

INTRODUCTION

Although human normal adult hemoglobin (Hb A) is one of the most well studied and well characterized proteins (Antonini and Brunori, 1971; Imai, 1982; Dickerson and Geis, 1983; Ho, 1992), the details of the molecular mechanism of the cooperative binding of oxygen to this molecule in vivo are not fully understood. A variety of effectors are known to influence the binding of oxygen to Hb A. Using nuclear magnetic resonance (NMR), a sensitive probe of molecular structure, we have previously conducted studies on purified Hb A in solution in the absence and presence of a variety of effectors and have investigated the binding of oxygen to the α- and β-chains of Hb A (Lindstrom and Ho, 1972; Johnson and Ho, 1974; Viggiano and Ho, 1979; Viggiano et al., 1979; Ho et al., 1982) and in lysed and intact red blood cells (Yao et al., 1986; Fetler et al., 1993). We have recently developed a new NMR technique that is well suited to obtaining quantitative measurements of the areas of ^{1}H-NMR resonances in the presence of a strong solvent resonance and other overlapping resonances (Fetler et al., 1993). This technique is used in the present work to measure the binding of oxygen to the α- and β-chains of Hb A in intact human red blood cells (erythrocytes) as a function of partial pressure of oxygen (pO_2). Studies of Hb A in red blood cells may serve as an intermediate step between studies of purified Hb A in vitro and of Hb A in tissue and, eventually, live animals and humans. From this study, we are able to obtain further information about the structural changes of Hb A upon the binding of oxygen in intact human red blood cells, and we can compare these results with our previous NMR studies on Hb A.

A review of NMR of hemoglobin has recently been given (Ho, 1992). ^{1}H-NMR resonances have been assigned to the hyperfine-shifted $N_\delta H$ protons of the proximal histidyl residues (F8) of the α- and β-chains of deoxyhemoglobin (deoxy-Hb A) at +63 and +76 ppm from 2,2-dimethyl-2-silapentane-5-sulfonate (DSS), respectively (Takahashi et al., 1980; La Mar et al., 1980), and to the ring current-shifted γ_2-CH_3 protons of the distal valine residues (E11) of both the α- and β-chains of oxyhemoglobin (HbO_2 A) at −2.4 ppm from DSS (Lindstrom et al., 1972; Lindstrom and Ho, 1973; Dalvit and Ho, 1985). The proximal histidyl

Received for publication 14 June 1994 and in final form 7 November 1994.

Address reprint requests to Dr. Chien Ho, Department of Biological Sciences, Carnegie Mellon University, 4400 Fifth Avenue, Pittsburgh, PA 15213-2683. Tel.: 412-268-3395; Fax: 412-268-7083.

Abbreviations used: NMR, nuclear magnetic resonance; DSS, 2,2-dimethyl-2-silapentane-5-sulfonate; Hb A, human normal adult hemoglobin; SUPERB-O, small flip-angle pulse sequences with a simultaneous uniform phase excitation region and binomial-type null with odd-order vanishing phase and amplitude coefficients; SUPERB-A, small flip angle pulse sequences with a simultaneous uniform phase excitation region and binomial-type null with all-order vanishing phase and amplitude coefficients; SUPERB-W, small flip-angle pulse sequences with simultaneous uniform phase excitation region and binomial-type null with wide bandwidth uniform phase excitation; PSIC, pulse shape-imperfection compensation; 2,3-DPG, 2,3-diphosphoglycerate; TEP, triethyl phosphate; FIDs, free induction decays; pH_i, intracellular pH; pH_e, extracellular pH; pO_2, partial pressure of oxygen; and pCO_2, partial pressure of carbon dioxide.

Dr. Fetler's present address: Varian Associates, 3120 Hansen Way, M/DS-317, Palo Alto, CA 94043.

0006-3495/95/02/681/13 $2.00

resonances of deoxy-Hb A are directly correlated with the paramagnetic shift caused by the heme iron in the oxygen-free hemoglobin and, thus, are expected to be a good measure of the oxygenation state of Hb A. In addition, the α- and β-chain proximal histidyl resonances are sufficiently resolved to monitor separately the binding of oxygen to the α- and β-chains of deoxy-Hb A. This information is not generally available by other techniques, such as optical spectroscopy. However, the distal valine resonances are sensitive to the conformation of the valine side chain in the heme pocket, and may or may not be directly correlated with the oxygenation state of Hb A. The distal valyl resonances from the α- and β-chains of HbO_2 A are not well resolved, even in purified Hb A (Lindstrom and Ho, 1973; Dalvit and Ho, 1985) and are further broadened in red blood cells. Both the proximal histidyl resonances and the distal valyl resonances are sufficiently isolated from most other ^{1}H-NMR signals to serve as marker resonances for the oxygenation state of Hb A inside intact red blood cells. Previous studies have been conducted in vivo using analogous ^{1}H-NMR resonances of deoxymyoglobin (deoxy-Mb) and oxymyoglobin (MbO_2) (Wang et al., 1990; Jue and Anderson, 1990; Kreutzer and Jue, 1991; Kreutzer et al., 1992). The technique that we use here provides spectra free of phase distortions. Thus, it is ideally suited for a quantitative analysis of ^{1}H-NMR resonances of proteins in the presence of an intense solvent peak and should find applications in in vivo ^{1}H-NMR spectroscopy.

MATERIALS AND METHODS

NMR methodology

The chief technical problem in selective excitation in in vivo ^{1}H-NMR spectroscopy is to suppress the water proton signal while simultaneously exciting the resonances of interest, and any significant neighboring resonances that border the region of interest, with uniform phase and amplitude, so that it is possible to measure accurately the areas of the resonances of interest. We have developed such a method utilizing pulse sequences (Fetler et al., 1993), which is the first method to use explicitly the small flip-angle approximation (Morris and Freeman, 1978; Hoult, 1979) to produce uniform phase excitation. The method is ideally suited to in vivo ^{1}H-NMR spectroscopy.

In brief, our method of selective excitation design is similar to the method used for the design of the binomial-pulse sequences (Hore, 1983), except that we eliminate the phase gradient over some region of the spectrum. We zero the derivatives of the excitation profile in two separate regions of the spectrum, such that good null characteristics are obtained in one region, with simultaneous good phase and amplitude characteristics in another region. The details of this method have previously been given (Fetler et al., 1993). For convenience, we refer to our previous *S*mall flip-angle pulse sequences with a simultaneous *U*niform *P*hase *E*xcitation *R*egion and *B*inomial-type null with *O*dd-order vanishing phase and amplitude coefficients (Fetler et al., 1993) as SUPERB-O(M_a, M_b), and with *A*ll-order vanishing phase and amplitude coefficients as SUPERB-A(M_a, M_b), where the integers M_a and M_b are the order of the highest-order vanishing derivatives of the transverse magnetization at offset frequencies $\Delta\omega = 0$ and $\Delta\omega = \pi/\tau$, respectively, where τ is the interpulse delay. Further details of this method are given in the Appendix.

We have made two improvements in the pulse sequence method that greatly enhance its performance. First, to quantify accurately the areas or intensities of the marker resonances, we wish to excite as wide a region as possible with uniform phase, including a particular set of resonances of interest, and any significant neighboring resonances whose wings overlap the resonances of interest. The SUPERB-O pulse sequences are adequate for exciting the marker resonances of deoxy-Hb A, because these resonances (at 63 and 76 ppm from DSS) are well isolated from most other ^{1}H-NMR resonances. In the absence of methemoglobin A (met-Hb A), the closest neighboring resonance, which is due to the hyperfine-shifted resonance of the β-chain of deoxy-Hb A, occurs at +23 ppm from DSS (Lindstrom and Ho, 1972; Johnson and Ho, 1974; Viggiano and Ho, 1979; Viggiano et al., 1979; Ho et al., 1982). However, the marker resonance for HbO_2 A that occurs at −2.4 ppm from DSS is much closer to the normally occurring range of ^{1}H-NMR chemical shifts, including the hyperfine-shifted resonances of deoxy-Hb A in the range −1 to −13 ppm from DSS, and many resonances of deoxy-Hb A and HbO_2 A in the range +5 to −2 ppm from DSS (Ho, 1992), with which it may overlap. We have found that the SUPERB-O and SUPERB-A pulse sequences are not ideally suited for observing the marker resonance for HbO_2 A, because it is difficult to achieve an increasingly wider uniform phase excitation bandwidth with this technique. On the other hand, by slightly modifying our design method, we are able to derive pulse sequences that cover a wide bandwidth, and that are also easier to produce experimentally. The details of this method, along with a brief summary of the general theory, are given in the Appendix. We refer to these pulse sequences by the acronym SUPERB-W (M_a, $[M_a + 2]\pi/N_f$), where "W" refers to *W*ide bandwidth uniform phase excitation, M_a is the highest-order vanishing derivative in the null region, and $[M_a + 2]\pi/N_f$ is the edge of the uniform phase excitation region, where N_f is the number of pulses in the pulse sequence. Two of these pulse sequences are shown in Table 1, and their small flip-angle excitation profiles are shown in Fig. 1. As with the SUPERB-O pulse sequences, we can control the magnetization in the null region, centered at $\Delta\omega = 0$ and in the uniform excitation region, centered at $\Delta\omega = \pi/\tau$, but we cannot specify the magnetization in a transition region between these two regions (i.e., $\Delta\omega\tau \sim 0.3\pi$ in Fig. 1). However, we may choose a pulse sequence such that the transition region is far from the region of interest.

Second, we now implement the pulse sequences experimentally using a method that compensates for imperfections in the nominally rectangular shape of the individual radio-frequency pulses. The rise and fall times of the pulses, as they are switched on and off, create significant pulse-shape imperfections and, thus, imperfections in the B_1 field. To compensate for this, we use a method similar to that used by Starčuk and Sklenář (1985). For our purposes, the general principles of this method may be stated as follows: each individual pulse in the pulse sequence may be decomposed into a series of sub-pulses, with lengths identical to another pulse or sub-pulse in the pulse sequence with opposite phase. The sub-pulses are separated by a delay d, which is short compared with the interpulse delay τ. An example of the pulse decomposition scheme is shown in Fig. 2. The original pulse sequence is given in Fig. 2 *A*. The pulses are grouped into a set of positive-amplitude pulses and a set of negative-amplitude pulses (Fig. 2 *B*), and each set is listed in a specific order. The first pulse length in the positive set is subtracted from the first pulse length in the negative pulse set; the remainder may then be subtracted from the next pulse of opposite sign. We continue this process until the last pulse is reached, which must be equal to the last difference in pulse lengths, because the sum of all the pulses is zero. This condition is

TABLE 1 SUPERB-W pulse sequences

A. SUPERB-W(0, $2\pi/5$)				
{0.1910,	0.3090,	0.3090,	0.1910,	−1.0000}
B. SUPERB-W(4, $6\pi/16$)				
{−0.1856,	−0.0904,	0.2542,	0.5036,	
0.3264,	−0.2436,	−0.7738,	−0.7826,	
−0.1778,	0.6156,	0.9758,	0.6022,	
−0.2130,	−0.8102,	−0.7062,	0.7054}	

The pulse sequences are given as a series of normalized pulse flip angles, $\{f_n\}$. Actual flip angles are given by $\theta_{tot}*\{f_n\}$, where θ_{tot} is the total flip angle desired at offset frequency $\Delta\omega = \pi/\tau$ in the excitation region (see Appendix). Time order of the pulses reads from left to right, starting with the upper left corner.

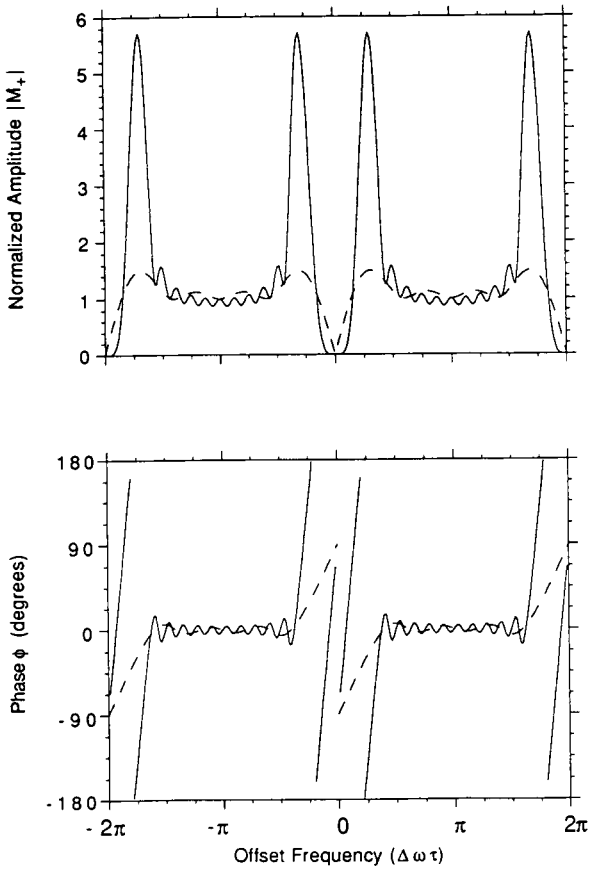

FIGURE 1 Excitation profiles of the SUPERB-W pulse sequences. Transverse excitation phase and amplitude are calculated in the small flip-angle limit (Eq. 3) and plotted against normalized offset frequency, $\Delta\omega\tau$. The flip-angle amplitude θ, or $|M_+|$, is normalized by dividing by θ_{tot} (see Eq. 3). (- - - -) SUPERB-W(0, $2\pi/5$); (——) SUPERB-W(4, $6\pi/16$).

guaranteed if we require at least a first-order null. We then replace the original pulses with the calculated lengths of the sub-pulses, keeping the pulses in the original time order (Fig. 2 *C*). The final pulse sequence may be referred to as the decomposition or the partition of the pulse sequence. For the purposes of sub-pulse calculation, the order of the pulses within the positive pulse set or within the negative pulse set may be rearranged in a variety of permutations, resulting in different experimental implementations of the same pulse sequence. Two simple schemes that we suggest are: (i) keeping the pulses in the original time order; and (ii) arranging the pulses from the shortest to the longest. All permutation schemes appear to be roughly equivalent experimentally. In general, one should use a small number of sub-pulses, because the effective length of the pulses in the final pulse sequence increases as the number of sub-pulse delays increases. One should also avoid extremely short pulses, which may sometimes be set to zero in actual implementation, because they are experimentally difficult to produce. We refer to the method of pulse-sequence decomposition as *P*ulse-*S*hape *I*mperfection *C*ompensation, or PSIC. The method is only effective if the carrier frequency and the null are both on resonance with the solvent, and it does not take into account imperfections in phase inversion between a positive and negative pair of pulses of identical length. This method is inherent to the odd-order antisymmetric binomial pulse sequences (Hore, 1983). In general, we find that, first, with a constant order null and increasing number of pulses, the residual water signal amplitude increases with the total pulse length, while the phase is approximately constant; second, with a constant number of pulses and increasing null order, the amplitude of the water signal generally decreases, although not monotonically, while the water signal phase changes in an unpredictable manner. These features are most likely due to the dynamics of the water magnetization during the pulse

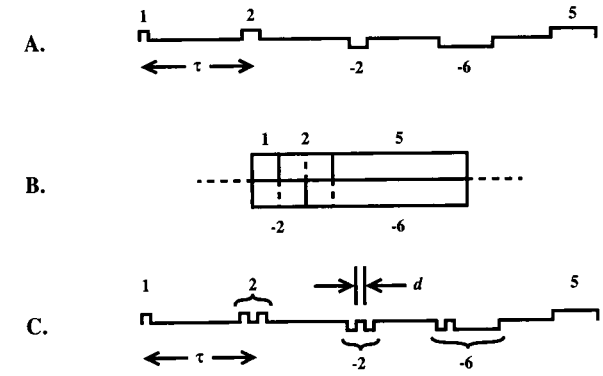

FIGURE 2 Pulse sequence decomposition scheme to produce pulse shape imperfection compensation (PSIC) for improved solvent suppression. The example is shown for the pulse sequence SUPERB-O(1, 3), or {1, 2, -2, -6, 5}. (*A*) Original pulse sequence with pulses of normalized flip angles $\{f_n\}$, with interpulse delay τ. (*B*) Decomposition of individual pulses into sub-pulse sequences by ordering the positive pulses and the negative pulses, and then subtracting them from each other successively in sequence. By permutation of the order of the pulses, a variety of decomposition schemes are possible (see text). (*C*) Actual experimental implementation of the pulse sequence, with sub-pulse delay d, $d \ll \tau$, which may be written {1,(1, 1), −(1, 1), −(1, 5), 5}.

sequence, either from radiation damping or from relaxation phenomena, which leaves the water with a small component in the *xy*-plane. In most cases, a pulse sequence implemented with PSIC (Fig. 2 *C*) is able to suppress the water signal by at least an additional order of magnitude, compared with the same pulse sequence without PSIC (Fig. 2 *A*), and thus is able to produce excellent water suppression in the null region. The PSIC method, in general, is not applicable to shaped-pulse methods, because of imbalances between positive and negative amplitudes in shaped-pulse generation.

With these two improvements, we have found that water signal suppression without saturation, along with reasonably uniform phase and amplitude excitation of the resonances within a specified bandwidth, is routinely feasible. An additional advantage of this method is that only a square-pulse generator with quadrature phase control is needed, so that it is not necessary to have a shaped-pulse (waveform) generator. We have written a FORTRAN computer algorithm that solves the set of equations for the pulse lengths using LU decomposition and back-substitution (Press et al., 1986), partitions the pulse sequence to compensate for pulse shape imperfections, calculates the interpulse delays by subtracting off half of the average pulse lengths, and then writes a pulse program in a format recognized by a Bruker AM series NMR spectrometer or a Varian NMR spectrometer with the VNMR operating system. Other formats are easily adaptable. This algorithm is especially useful for the longer pulse sequences, for which the calculations become lengthy.

Sample preparation

Samples of deoxy-Hb A and carbonmonoxyhemoglobin A (HbCO A) in 0.1 M phosphate buffer, for tests on Hb A in solution, were prepared from blood samples obtained from the Central Blood Bank of Pittsburgh, as previously described (Lindstrom and Ho, 1972, 1973). HbCO A was used as an analog to HbO_2 A for tests of ¹H-NMR pulse sequences and was found to be adequate for testing, although the analogous marker resonance for HbCO A occurs at −1.8 ppm from DSS, rather than at −2.4 ppm from DSS for HbO_2 A (Lindstrom and Ho, 1973; Dalvit and Ho, 1985). We conducted studies on both fresh erythrocytes, for which the concentration of 2,3-diphosphoglycerate (2, 3-DPG), a major effector of Hb A oxygen binding (Benesch and Benesch, 1967; Chanutin and Curnish, 1967), is significant, and on erythrocytes stored until 2,3-DPG was depleted. For experiments on fresh erythrocytes, blood was obtained from volunteers by venipuncture using a 6-ml collection tube with 1-ml acid-citrate-dextrose (ACD) solution

B (Becton Dickinson, Vacutainer 4816), which helps to maintain the energy state of the cells and also decreases pH. For experiments on 2,3-DPG-depleted blood, blood was collected using a 10-ml heparinized collection tube (Becton Dickinson, Vacutainer 6480) and stored at 4°C for 5–8 days before sample preparation, during which time the pH decreased, because of changes in metabolite levels. All blood was initially kept on ice for 30 min immediately before sample preparation. During sample preparation, the samples were kept as cold as possible to prevent degradation, and especially to maintain the concentration of 2,3-DPG. Whole blood was used for all experiments, without washing the cells, to minimize sample degradation during handling. Triethyl phosphate (TEP) (Aldrich Chem Co., Milwaukee, WI) was added to all samples for a final concentration of 1.0 mM as an internal ^{31}P-NMR chemical shift reference (Kirk and Kuchel, 1988). All chemicals used were of reagent grade and were used without further purification. To obtain partially oxygenated samples between approximately 50 and 100% oxygen saturation, blood removed directly from the Vacutainer tubes with TEP added was either mixed with fully oxygenated blood in appropriate volumes or was injected with 0.1–0.5 ml of pure oxygen gas after nitrogen-gassing the NMR tube. To obtain fully oxygenated samples, blood was incubated in a tonometer (Instrumentation Laboratories, IL 237), maintained at 5–7°C with a cold water bath, for 1 h under a gas mixture of 95% O_2/5% CO_2 and transferred into an oxygen-gassed 5-mm NMR tube. To obtain partially oxygenated blood samples between approximately 0 and 50% oxygen saturation, blood removed directly from the Vacutainer tubes with TEP added was incubated in the tonometer at 5–7°C for varying lengths of time up to 3 h, under a gas mixture of 95% N_2/5% CO_2. Samples were withdrawn from the tonometer into a sealed nitrogen-gassed NMR tube. For the fresh blood samples, 295 mM D-glucose (Fisher) was also added to blood in a volumetric ratio of 1:10 immediately before preparation of partially oxygenated states, to further help maintain the energy state of the cells. To obtain a single sample with complete removal of oxygen for each data set, a deoxygenated solution of 20 mM sodium dithionite, prepared from solid sodium dithionite (Fluka), and 275 mM D-glucose was added to the fully nitrogen-gassed sample for a final dithionite concentration of ~1 mM. Dithionite has been used both for samples of aqueous Hb A (Antonini and Brunori, 1971; Englander et al., 1987) and for erythrocyte studies (Gasparovic and Matwiyoff, 1992), but it may cause oxidative stress to the cells. All NMR samples were stored at 4°C after preparation, for between 30 min and 2 and 1/2 days. Immediately before the NMR experiments, the NMR tubes were centrifuged in a specially designed rotor chamber in an open-top centrifuge (Sorvall, SS-1) at 20–22°C for 30 min at 2000 rpm to pack the cells, to avoid the effects of cell settling during the experiments, and to avoid microscopic magnetic susceptibility gradients (Fabry and San George, 1983). We found that this was a sufficiently low speed that our 5-mm NMR tubes (Norell, 507-HP) did not break, and resulted in a sample volume of 0.3–0.6 ml of packed cells in the NMR tube. The concentration of Hb A in packed cells was thus approximately constant. ^{1}H chemical shifts were measured relative to water at 29°C, which was then referenced to DSS, which is 4.76 ppm upfield from water. During the time of sample preparation and storage, the 2,3-DPG concentration of the fresh samples decreased by no more than 30% of its initial value at venipuncture. The 2,3-DPG-depleted samples were stored at 20–22°C for an additional 8–14 h after sample preparation, and before centrifugation, to further deplete 2,3-DPG, and were stored at 4°C for at least 30 min before centrifugation. Each set of experiments, prepared from the same individual, consisted of 8–10 NMR samples and took 3 days to run. The samples in each set of experiments were run in a pseudo-random order with respect to percent oxygenation. Five sets of experiments were run for fresh blood, and two were run for 2,3-DPG-depleted blood.

NMR experiments

All NMR experiments were performed on a Bruker AM-300 spectrometer operating at a proton frequency of 300 MHz, using a 5-mm broad band probe, for which the decoupling coil was used for both proton excitation and detection. Spectral excitation profiles of each pulse sequence were obtained using a sample of 2% H_2O/98% D_2O doped with copper sulfate and were obtained by repetition of the experiment with the carrier frequency incremented at uniformly spaced values and summing the free induction decays (FIDs). Each blood sample was allowed to equilibrate in the magnet at 29°C for 15 min and was maintained at that temperature throughout the experiment. The pulse sequence SUPERB-O(2, 1), using a total flip angle of 70°, with interpulse delay τ of 25.6 μs, and using PSIC with a sub-pulse delay d of 1.5 μs, was implemented for detection of the marker resonances of deoxy-Hb A. This pulse sequence is essentially a $\{1, -3, 3, -1\}$ (Hore, 1983) with an extra pulse to refocus the phase. The pulse sequence amplitudes may be written $\{29, -48, -30, 88, -39\}$. The 90° pulse length was adjusted to 23 μs for each sample. A delay of 1.4τ, or $x = 1.4$ (see Appendix), was also added to the end of the pulse sequence, so that the phase difference between the marker resonance and the deoxy-Hb A resonance at 18 ppm is actually 360°, to minimize baseline distortion in the region of interest. Although this is really a semi-soft pulse sequence, due to limited radio-frequency power, the excitation profile was found to be adequate. Because the relaxation times of these resonances are short (Yao et al., 1986), we collected 10,000 scans in 4 min and repeated this measurement 6 times for each sample. The carrier frequency was alternately set on resonance with the water proton signal and 50 Hz upfield from the water resonance. The residual water signal phase and amplitude were found to be the same, on average, for both carrier frequencies. Careful shimming of the samples was necessary to avoid obtaining interfering signals from solid components inside the probe, which are apparent on the chemical shift range of this experiment. The pulse sequence SUPERB-W(4, 6π/16) (Table 1), using a total flip angle of 90°, and 90° pulse length of 52 μs, with interpulse delay τ of 235 μs and sub-pulse delay d of 5 μs, was implemented for detection of the HbO_2 A marker resonance, which is 7.1 ppm upfield from the water resonance, or 2.4 ppm upfield from DSS. The 90° pulse length was adjusted to 52 μs for each sample. This pulse sequence excites resonances from 2.6 to 11.6 ppm upfield from water with uniform phase. We collected 2048 scans in 20 min and repeated this measurement twice. After the ^{1}H-NMR experiments, the proton decoupler was turned on for 15 min to allow for temperature equilibration to 30°C. A ^{31}P-NMR experiment was then run with continuous proton decoupling using a 70° flip angle, collecting 256 scans in 7 min. Total time for the NMR experiments was ~2 h. Concentration of 2,3-DPG was estimated by ^{31}P-NMR intensities of the C2 and C3 phosphate groups, correlated with enzymatic assay (Sigma, 35-UV). All samples showed at least a small buildup in inorganic phosphate. Intracellular pH (pH_i) was calculated from inorganic phosphate chemical shift using a pH titration of fully oxygenated lysed red blood cells using sodium NaOH and HCl, measured by pH electrode (Radiometer, PHM 64). Measuring the ^{31}P chemical shift and pH of 4.5 mM potassium phosphate and 3.0 mM TEP at 21 and 37°C, and based on previous work (Lam et al., 1979; Tehrani et al., 1982; Fabry and San George, 1983; Labotka, 1984), for a pH range of 6.7–7.5 (results not shown), we have estimated the pH as follows

$$\mathrm{pH} = 4.7919 + 0.0076\,\delta, \quad (1)$$

where δ is the inorganic phosphate chemical shift (in Hz) at 30°C, at 121.5 MHz for ^{31}P-NMR measurements. ^{31}P chemical shifts were measured relative to TEP, which was then referenced to 85% H_3PO_4.

Post-NMR analysis

Immediately after the NMR experiments, the samples were stored for up to 6 h at 4°C. For each sample, the packed red-cell component was then remixed with the plasma fraction by inversion within the NMR tube. The samples were then transferred into a nitrogen-gassed glove bag, where a portion of the sample was drawn into a nitrogen-gassed syringe. Blood-gas analysis (Radiometer, ABL2) was then performed on the sample, for which partial pressure of oxygen (pO_2), partial pressure of carbon dioxide (pCO_2), and extracellular pH (pH_e) were measured. The blood-gas measurements were performed at 37°C and then calibrated to 30°C using calibration curves. Each of these samples was also analyzed for the content of HbO_2 A, deoxy-Hb A, HbCO A, and met-Hb A using optical measurements (Instrumentation Laboratories, IL 282).

RESULTS

The average characteristics of the blood samples are given in Table 2. By optical methods, the contents of met-Hb A and HbCO A were found to be within normal values: no met-Hb A was found, and HbCO A was 1–2% of total Hb A. The average partial pressure of carbon dioxide, pCO_2, was found to be 60 mmHg, slightly elevated from average normal conditions (Winslow et al., 1977). For several samples, ^{31}P-NMR experiments were run before and after the ^{1}H-NMR experiments, and a decrease of less than 10% was observed in the 2,3-DPG intensities during the NMR experiments. No differences were observed in the average characteristics of male and female subjects (results not shown). This is expected, because the variation in concentration of 2,3-DPG between samples is primarily due to differences in sample preparation and correlates roughly with sample-preparation time. Only one peak for inorganic phosphate was observed in all samples and was assumed to be the intracellular component, because the cells were packed. The average intracellular pH values, in comparing the fresh and 2,3-DPG-depleted erythrocytes, are within statistical error of each other (Table 2), as are the extracellular pH values, which allows for direct comparison of the fresh and 2,3-DPG-depleted samples. The closeness of pH is due primarily to sample preparation methods: the fresh samples were collected in Vacutainer tubes with ACD, which lowers the pH; the 2,3-DPG-depleted samples were collected in heparinized tubes, and during storage the pH of the heparinized samples decreases because of changes in metabolite levels. Comparison of pH between samples shows a slight correlation with sample preparation time, decreasing with time. There is a further drop in pH of ~0.06 in the fully deoxygenated samples with dithionite added. Given the pH distribution of our samples, and within our margins of error, the alkaline Bohr effect has no measurable effect on the oxygenation curve, which would be most apparent at low partial oxygen pressure (Antonini and Brunori, 1971). Intracellular pH in packed erythrocytes, as estimated from inorganic phosphate chemical shift, was consistently lower than extracellular pH, as measured from resuspended whole blood, by ~0.20, both in fresh and 2,3-DPG-depleted samples, in agreement with previous values (Sachs et al., 1975; Lam et al., 1979; Tehrani et al., 1982). The error between samples in the pH gradient, ΔpH, is smaller than the error in the average intracellular and extracellular pH values, because erythrocytes maintain a pH gradient with respect to their environment. The variation of pH between samples is primarily due to differences in sample preparation.

The excitation profile of the pulse sequence SUPERB-O(2, 1) with $x = 1.4$ (see Appendix), suitable for observing the ^{1}H-NMR marker resonances of deoxy-Hb A, is shown in Fig. 3. Tests were run with this pulse sequence with varying repetition times between 20 and 1000 ms (results not shown), and it was found that the residual water signal did not significantly vary in phase or amplitude, so that saturation of the water signal due to the short repetition time did not significantly contribute to water suppression. Observation of deoxy-Hb A inside fresh packed erythrocytes of samples of varying oxygenation state is also shown in Fig. 3. A second-order polynomial baseline is subtracted from the erythrocyte spectra. The main contribution to the variation in baseline is a slight variation in phase and amplitude of the water signal. The excitation profile of the pulse sequence SUPERB-W(4, $6\pi/16$) and observation of HbO_2 A inside fresh packed erythrocytes of varying oxygenation state are shown in Fig. 4. Erythrocyte spectra are shown after first-order polynomial

TABLE 2 Average characteristics of erythrocyte samples

Characteristics*	Fresh samples	2,3-DPG-depleted samples
2,3-DPG‡	3.7 ± 0.7 mM	0.4 ± 0.4 mM
pH_e§	7.06 ± 0.07	7.14 ± 0.06
pH_i‡	6.86 ± 0.07	6.94 ± 0.05
$\Delta pH = pH_e - pH_i$	0.20 ± 0.02	0.20 ± 0.02

*All measurements are reported at 30°C. The SD is given.
‡Measurements performed on packed erythrocytes using ^{31}P-NMR, performed immediately after ^{1}H-NMR measurements.
§Measurements performed on whole blood, using blood-gas methods (Radiometer, ABL2).

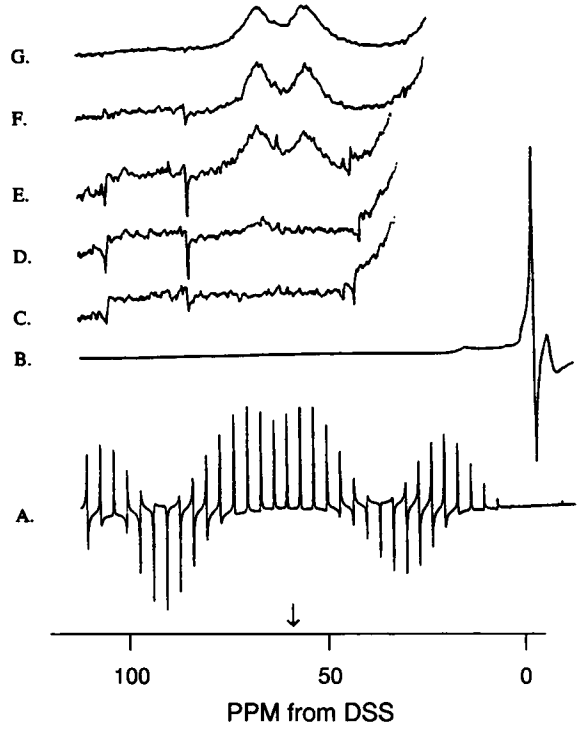

FIGURE 3 Experimental results obtained using pulse sequence SUPERB-O(2, 1) with added delay 1.4τ, suitable for observing the ^{1}H-NMR marker resonances, hyperfine-shifted, exchangeable $N_\delta H$ of proximal histidyl residues of deoxy-Hb A, at +63 ppm (α-chain) and +76 ppm (β-chain) from DSS. (*A*) Pulse sequence profile obtained with test sample of $H_2O/D_2O/CuSO_4$. Arrow indicates approximate center of uniform phase excitation region. (*B–G*) Spectra of fresh packed erythrocyte samples: (*B*) 0% oxygenation (fully deoxygenated sample), vertical scale expansion × 1; (*C*) 100% oxygenation, scale × 250; (*D*) 97% oxygenation, scale × 250; (*E*) 85% oxygenation, scale × 250; (*F*) 50% oxygenation, scale × 100; (*G*) 0% oxygenation, scale × 50. All erythrocyte spectra were processed with no more than second-order polynomial baseline correction. Good water signal suppression was achieved using pulse shape imperfection compensation (PSIC).

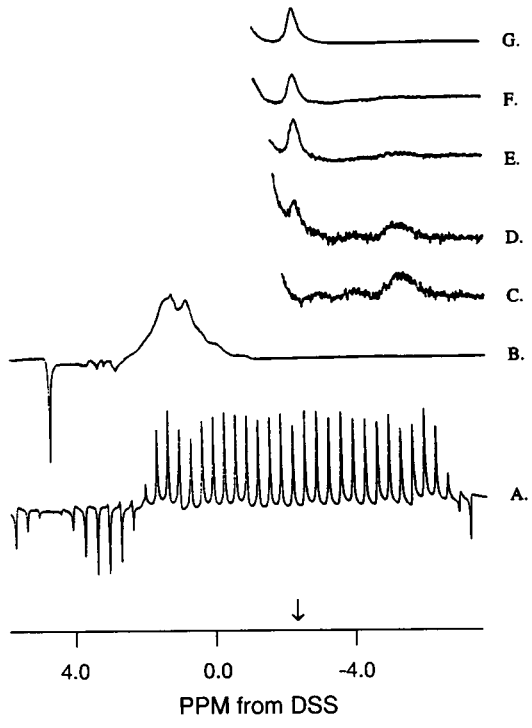

FIGURE 4 Pulse sequence SUPERB-W(4, $6\pi/16$), suitable for observing ^{1}H-NMR marker resonance of HbO_2 A, the ring current-shifted γ_2-CH_3 of E11 Val, at -2.4 ppm. (*A*) Pulse sequence profile obtained with test sample of $H_2O/D_2O/CuSO_4$. Arrow indicates center of uniform phase excitation region. (*B–G*) Spectra of fresh packed erythrocyte samples: (*B*) 100% oxygenation, vertical scale expansion × 1; (*C*) 0% oxygenation, scale × 250; (*D*) 3% oxygenation, scale × 250; (*E*) 20% oxygenation, scale × 100; (*F*) 34% oxygenation, scale × 50; (*G*) 100% oxygenation, scale × 25. All spectra were processed with only first-order baseline correction. Good water signal suppression was achieved using pulse shape imperfection compensation (PSIC). Accurate peak area estimation is possible, because of the excellent phase excitation characteristics of the SUPERB-W(4, $6\pi/16$) pulse sequence.

baseline correction. The uniform phase excitation bandwidth is wide enough to cover most resonances that significantly overlap the marker resonance.

It is apparent that the hyperfine-shifted, exchangeable $N_\delta H$ resonances of the proximal histidyl residues of the α- and β-chains of deoxy-Hb A overlap each other in the spectra of erythrocytes. We wish to estimate the area of each resonance separately so that we may compare the degree of saturation of the α- and β-subunits of hemoglobin. To interpret quantitatively these spectra, we fit them using the sum of two Lorentzian lines, plus a third-order polynomial for the baseline

$$S(\omega) = \frac{m_\alpha T_{2\alpha}}{[1 + T_{2\alpha}^2(\omega_\alpha - \omega)^2]} + \frac{m_\beta T_{2\beta}}{[1 + T_{2\beta}^2(\omega_\beta - \omega)^2]} + \sum_{i=0}^{3} p_i \omega^i. \quad (2)$$

$S(\omega)$ is the magnetization as a function of offset frequency ω, m_α and m_β are the amplitudes, $T_{2\alpha}$ and $T_{2\beta}$ are the transverse relaxation times, ω_α and ω_β are the resonant frequencies of the proximal histidine resonances of the α- and β-chains of deoxy-Hb A, respectively, and p_i is the ith polynomial coefficient. Curve-fitting of Lorentzian lines is typically difficult to implement; however, we may use previous knowledge of these resonances to aid the curve-fitting process. Inspection of the data reveals that the resonance positions (ω_α and ω_β) and transverse relaxation times ($T_{2\alpha}$ and $T_{2\beta}$) are constant. We have found 141 μs for $T_{2\alpha}$ and 137 μs for $T_{2\beta}$ in packed erythrocytes. We also know that the excitation phases are constant and equal to zero, as given in Eq. 2. Hence, we may hold these parameters constant and fit the amplitudes, m_α and m_β, and the baseline polynomial coefficients, $\{p_i\}$. The areas, A and B, of the α- and β-chain resonances of deoxy-Hb A, are given by $\pi m_\alpha/T_{2\alpha}$ and $\pi m_\beta/T_{2\beta}$, respectively. We use only a limited frequency range (12.0–24.9 kHz) to avoid a noise spike at 25.2 kHz from the carrier and also to allow for better modeling of the baseline by a third-order polynomial.

An example of a fitted spectrum of fresh, fully deoxygenated erythrocytes is shown in Fig. 5. The same spectrum, with the baseline subtracted, is also shown along with the fits of the individual Lorentzian functions. It is possible that the

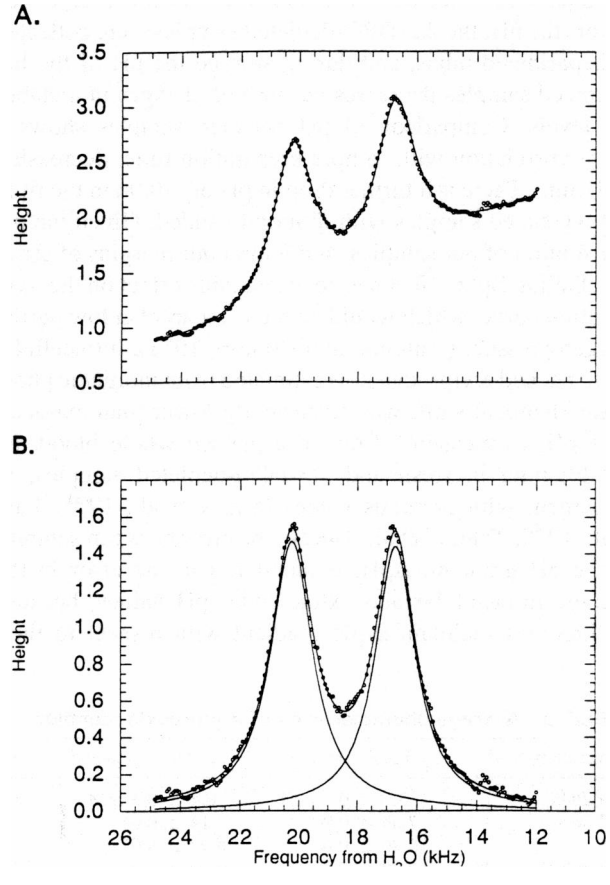

FIGURE 5 (*A*) Typical spectrum of fresh fully deoxygenated erythrocytes (○). A curve fit of the spectrum using Eq. 2 is also shown (——). The amplitude scale is arbitrary. (*B*) Spectrum of fresh fully deoxygenated erythrocytes after subtraction of polynomial baseline calculated from the curve fit (○), compared with Lorentzian lines calculated from the curve fit (——).

curve-fitting process leads to systematic errors in the area estimation, which may be true if the polynomial part of the fitting function subtracts off part of the Lorentzian lineshapes as well as the baseline. However, examination of the χ^2 surface (Bevington and Robinson, 1992) with respect to the fitting variables shows that the baseline parameters vary independently from the positions and linewidths of the resonances (see Eq. 2). Variations in the phase of the water signal appears to be the major source of variance in the baseline parameters.

To calibrate the areas of the hyperfine-shifted, exchangeable $N_\delta H$ resonance of the proximal histidyl resonances of the α- and β-chain resonances of deoxy-Hb A, we must also take into account any possible difference in the excitation and detection of the two resonances. First, the total excitation flip angle may differ between the two resonances, slightly favoring the α-chain resonance. Second, the difference between the T_2 relaxation times of the two resonances also matters, because the total pulse-sequence length is approximately equal to T_2 in erythrocytes; this also slightly favors the α-chain resonance. Third, the difference in the T_1 relaxation times of the two resonances may count, because the repetition time is approximately twice T_1. However, we find it difficult to obtain a reliable enough value for T_1 in erythrocytes to estimate the preference for the α- or β- chains in packed erythrocytes. In solution, this effect slightly favors the β-chain resonance. Based on all three factors, we estimate that there is no net bias in estimating the area of the two markers. The β-chain resonance appears to be larger than the α-chain resonance for all samples in which deoxy-Hb A was detectable, including both the fresh and 2,3-DPG-depleted samples. This is clearly illustrated in the spectrum obtained at high percent oxygen saturation (Fig. 3 *D*), where the β-chain resonance is barely visible above the noise, but the α-chain resonance is not visible at all. The figure of 97% oxygenation quoted was arrived at by integrating the relevant portion of the spectrum using the integration routine of the standard DISR89 package and is only qualitative.

The areas of the deoxy-Hb A marker resonances, *A* and *B*, for both fresh and 2,3-DPG-depleted samples, are shown in Fig. 6 as a function of partial pressure of oxygen, pO_2, measured on resuspended erythrocytes. The areas are normalized such that the total peak area is 100% at full deoxygenation. The values of pO_2 measured by blood-gas analysis (ABL2) may indicate too much oxygen in the samples by up to 5 mmHg, which may have entered into the sample during injection, and we report the values as measured. From six repetitions of the same experiment on the same sample, the SD in the areas, *A* and *B*, is 3% of the total oxygen saturation for each data point above 10% total deoxy-Hb A. However, the error in the saturation curve due to sample to sample variation is as much as 5% of the total oxygenation The difference between the two areas, $(B - A)$, is represented in Fig. 7, which shows that a maximum difference of between 3 and 10% is reached at ~10 mmHg, and is roughly constant up to the maximally obtainable deoxygenation. The oxygen saturation of hemoglobin as measured by the decrease in the

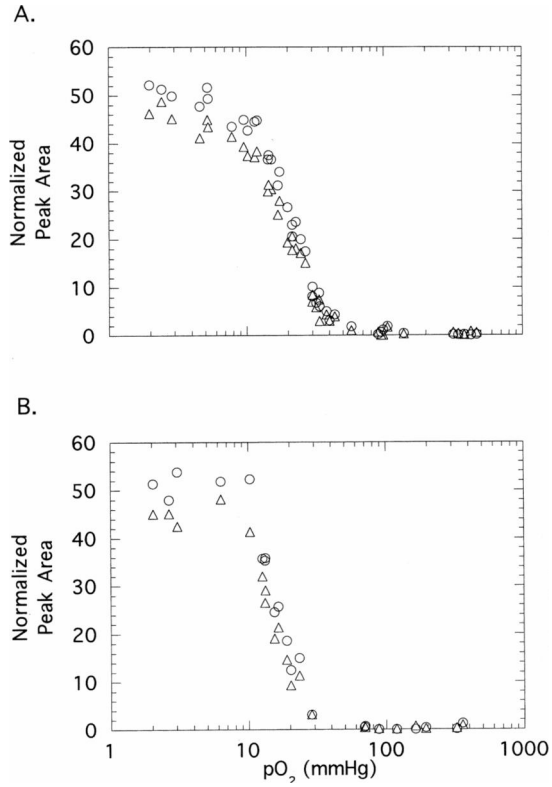

FIGURE 6 Normalized areas of the deoxy-Hb marker resonances in erythrocytes A (△) and *B* (○) from the individual α- and β-chains, respectively, obtained from curve fits (Eq. 2; Fig. 5) as a function of partial pressure of oxygen (pO_2): (*A*) fresh samples; (*B*) 2,3-DPG-depleted samples. Each data point represents the average of six measurements. Margins of error are not shown, for clarity.

sum of the two resonances, $Y_{AB} = [100\% - (A + B)]$, is shown in Fig. 8. The SD in the sum and difference of *A* and *B* is also 5% of the total oxygen saturation for all data points above 10% total deoxy-Hb A, because the errors in the areas *A* and *B* are correlated. Hb A oxygen saturation, as measured by optical methods (IL 282), is also shown in Fig. 8 for comparison. The optical measurements may overestimate the oxygen saturation by as much as 3% of the full oxygenation, due to oxygen entering the samples during sample injection.

For the HbO_2 A marker resonance, we may estimate the peak area by integration of the digitized spectrum. Fitting a spectrum to a function with multiple Lorentzian lines in this case is difficult, because there are many resonances that overlap the resonance of interest and are not well resolved. The region of uniform phase excitation covers the HbO_2 A resonance, and resonances that occur in the region +1.7 to −6.5 ppm from DSS (or 3.0–11.2 ppm upfield from water) from hyperfine-shifted resonances of deoxy-Hb A and from other resonances that occur in both HbO_2 A and deoxy-Hb A downfield from the HbO_2 A marker resonance (Ho, 1992). Other resonances occur downfield of +1.7 ppm from DSS and are excited with different phase but are far enough away not to overlap the HbO_2 A marker resonance. Chemical shifts, and T_1 and T_2 relaxation times of some of the potentially overlapping resonances, are given in Table 3. T_1 was

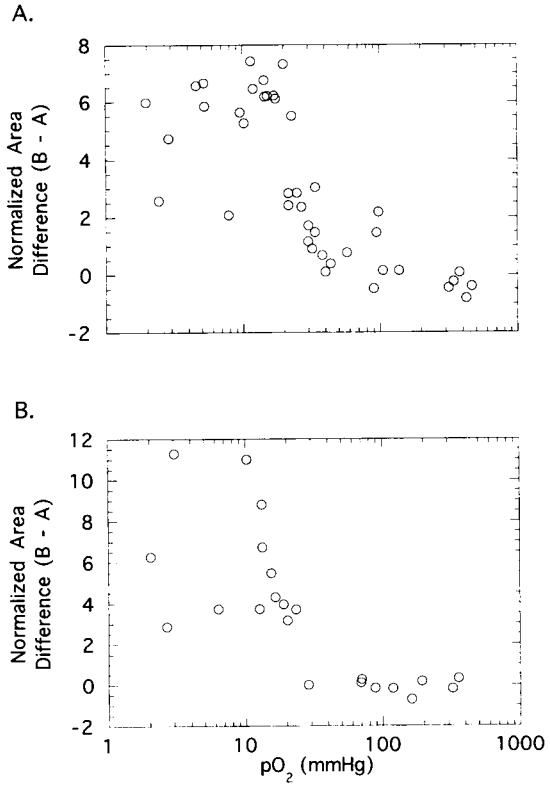

FIGURE 7 Difference, $(B - A)$, between the normalized areas of the deoxy-Hb marker resonances of the α- and β-chains of Hb A in erythrocytes as obtained from curve fits (see Fig. 5), as a function of partial pressure of oxygen (pO_2). Areas are normalized such that $A + B = 100\%$ at full deoxygenation: (A) fresh erythrocytes; (B) 2,3-DPG-depleted erythrocytes. Each data point represents the average of six experiments. Margins of error are not shown, for clarity.

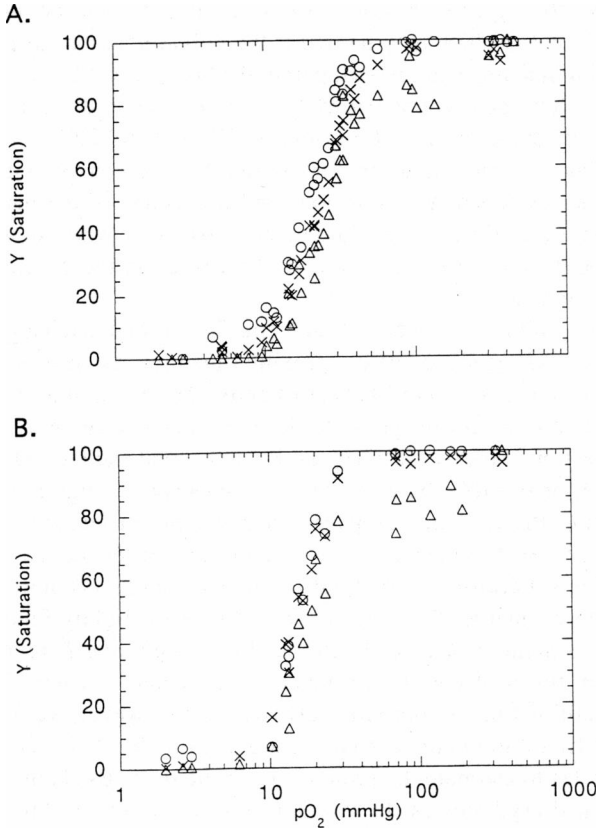

FIGURE 8 Comparison of the oxygenation of Hb A in erythrocytes, as a function of partial pressure of oxygen, pO_2, measured by different techniques: (A) fresh erythrocytes; (B) 2,3-DPG-depleted erythrocytes. Methods of measurement are as follows: Y_{AB} (○), calculated from the decrease in the areas, A and B, of the deoxy-Hb A marker resonance, as calculated from the normalized curve fits (see Fig. 5); spectrophotometry (×); R (Δ), area of the HbO_2 A marker resonance, obtained by digital integration.

measured by inversion-recovery (Carr and Purcell, 1954; Meiboom and Gill, 1958), and T_2 was calculated from Lorentzian linewidths. The values are reported for purified Hb A in aqueous solution and may be shorter in erythrocytes because of increased viscosity.

The main problem is estimating the area of the HbO_2 A resonance in the presence of overlapping resonances. We consider the other resonances only as far as they contribute to the baseline of the HbO_2 A marker resonance. The baseline is chiefly due to neighboring resonances, excited with the same phase by the SUPERB-W pulse sequence. Variations in the phase and amplitude of the water signal are the major source of variations in baseline. Curve-fitting with Lorentzian lines is impractical in this case of multiple overlapping resonances. Instead, we chose to estimate the baseline manually by a second-order polynomial function and measure the area by digital integration, using the integration subroutine of the DISR89 NMR package provided with the spectrometer. Contributions from the deoxy-Hb A resonances in this region become significant at low percent oxygenation. However, because the total length of the pulse sequence is 3.8 ms, the broader lines are selectively attenuated based on their shorter T_2. The T_2 relaxation times of these resonances in erythrocytes are even shorter than those given in Table 3. The repetition time is about twice T_1 of the HbO_2 A resonance, so that T_1 attenuation is not severe for this resonance. Measurements at very high partial pressures of oxygen are necessary to obtain a good representation of the upper part of the

TABLE 3 T_1 and T_2 measurements of Hb A resonances in the ^{1}H-NMR chemical shift range 0.0 to −7.0 ppm from DSS

Chemical shift δ (ppm)	T_2 (ms)	T_1 (ms)
−0.05*	5.3	280
−0.35*	6.4	230
−0.85*	6.4	130
−1.35*	4.0	88
−1.80*	7 ± 3	45
−2.08*	5.3	45
−2.41‡	5.9	202
−2.66*	2.7	79
−3.02*	2.7	86
−4.14*	1.1	83
−5.17*	1.5	81
−6.7*	0.94	§

*From deoxy-Hb A in 0.1 M phosphate, pH 7.0, 29°C. See also Ho (1992).
‡Resonance that serves as marker for HbO_2 A, from HbO_2 A in 0.1 M phosphate, pH 7.0, 29°C.
§In T_1 measurements, the intensity of this resonance was too small to quantify accurately.

curve. We assign a value of 100% oxygen saturation to the area of the HbO_2 A marker resonance of the fully oxygenated sample and refer to the normalized area of this resonance as R. The limits of the integrated region assigned to the area of this resonance varied with percent oxygenation. The SD of R is 5% of total oxygen saturation of Hb A at oxygenation greater than ~20% from two repetitions of each experiment. However, the error in R can be as much as 10% of the full oxygenation, because of variation between samples. The error may be greater at less than ~20% oxygenation, because of the presence of overlapping resonances of deoxy-Hb A. However, the HbO_2 A marker resonance is still visible above the background at 3–5% oxygenation (Fig. 4 D). The figure of 3% oxygenation should only be considered as a qualitative estimate. The signal falls below the noise level or is obscured by overlapping deoxy peaks for pO_2 less than ~15 mmHg. Nevertheless, Fig. 4 D illustrates the potential of the SUPERB pulse sequence. Fig. 8 shows the normalized area, R, inside fresh and 2,3-DPG-depleted packed red blood cells, as a function of partial oxygen pressure, measured on resuspended samples.

TABLE 4 Characteristics of Hb A oxygen binding in packed erythrocytes

Method	2,3-DPG	p_{50} (mmHg)*	n_{max}‡
Deoxy-Hb A Resonances§	+	19.3 ± 2.0	2.7 ± 0.3
Deoxy-Hb A Resonances§	−	15.4 ± 2.0	2.9 ± 0.3
HbO_2 A Resonance†	+	28.2 ± 2.0	2.9 ± 0.3
HbO_2 A Resonance†	−	18.4 ± 2.5	2.7 ± 0.7
Optical Measurements, Hb A¶	−	11.0	2.9
Optical Measurements, WholeBlood‖	+	28.8 ± 0.3	2.6 ± 0.1

*p_{50} is the partial pressure of oxygen at 50% saturation.

‡The maximum Hill coefficient, n_{max}, is the maximum value of $\partial\log[y/(1-y)]/\partial\log p$, where y is the oxygen saturation and p is the partial oxygen pressure.

§Calculated from the areas, A and B, of the respective ¹H-NMR resonances of α- and β-chains of deoxy-Hb A, from lineshape fitting of the resonances. p_{50} and n_{max} were calculated from the total Hb A saturation, $Y_{AB} = 100\% - (A + B)$.

†Calculated from the area, R, of the HbO_2 A marker resonance estimated by computerized digital integration.

¶Data taken from Antonini and Brunori (1971). Hb A (15 μM) is stripped of phosphates, in 0.2–0.4 M NaCl, pH 7.2, at 30°C.

‖Data taken from Winslow et al. (1977). Hb A saturation measurements were made by spectrophotometry, under conditions pH 7.42, 37°C, molar ratio of 2,3-DPG to Hb A 0.89, pCO_2 40 mm Hg.

DISCUSSION

Saturation characteristics

The oxygen saturation of hemoglobin, as measured by the decrease in the deoxy-Hb A marker resonances of packed erythrocytes, Y_{AB}, is in close agreement with the spectrophotometric measurements on resuspended samples, within the margin of error. The areas of the two resonances, A and B, are not equal at the lowest partial oxygen pressures (Figs. 6 and 7), suggesting that complete deoxygenation of the samples has not been achieved. Previous studies indicate that it is difficult to achieve full deoxygenation in erythrocyte suspensions (Gasparovic and Matwiyoff, 1992). In our experiments, there appears to be no difference between maximally nitrogen-gassed samples with and without sodium dithionite. It is also possible that the curve-fitting process leads to a systematic error in the area estimation or that the excitation of the two resonances is not the same. As previously discussed, examination of the χ^2 surface (Bevington and Robinson, 1992) shows that the former possibility is not true, whereas the latter possibility may contribute up to a few percent difference. Because of the close agreement with optical measurements, it appears that Y_{AB} is a reliable indicator of Hb A oxygenation, and any miscalibration of the total deoxy-Hb A peak area is at most a few percent. On the other hand, the saturation measured by the increase in the HbO_2 A marker resonance appears to deviate from both the other measurements of Hb A oxygen saturation.

The 50% saturation point, p_{50}, and the maximum value of the Hill coefficient, n_{max}, of the oxygen-binding curves, calculated from the total oxygen saturation measured by NMR, Y_{AB} and R, are given in Table 4. The binding curves, as indicated by Fig. 8 and by the characteristics in Table 4, qualitatively fall where expected for the experimental conditions and effectors present. The effectors generally are not additive, and their effects may compete with each other, so it is difficult to assess quantitatively the relative contributions of the various effectors in the erythrocytes. However, our results agree qualitatively with our earlier results on Hb A in vitro in the presence of various effectors. As expected, comparison of our fresh and 2,3-DPG-depleted samples indicates that 2,3-DPG is a more potent effector of oxygen binding than the other effectors, as indicated by shifts in the oxygen saturation curves of both Y_{AB} and R. Although there is an increase in P_i in the 2,3-DPG-depleted samples, its effect on oxygen binding in our samples is apparently small compared with that of 2,3-DPG; this is in agreement with studies on Hb A in vitro (Benesch and Benesch, 1967; Chanutin and Curnish, 1967; Imai, 1982). Comparing Y_{AB} with spectrophotometric measurements in stripped Hb A, p_{50} is increased in the 2,3-DPG-depleted case and is increased further still in the fresh erythrocyte case for all our methods of saturation measurement. We attribute this primarily to the effects of 2,3-DPG, a major effector in human erythrocytes. In the 2,3-DPG-depleted case, there also may be an effect of P_i that results from the breakdown of 2,3-DPG. A variety of other effectors are known to influence the oxygen binding in human red cells (Bunn et al., 1971; Antonini and Brunori, 1971; Hamasaki and Rose, 1974; Gupta et al., 1978; Viggiano and Ho, 1979; Viggiano et al., 1979; Ho et al., 1982; Craescu et al., 1986; Wodak et al., 1986). Comparison of the fresh packed erythrocytes with previous experiments on fresh blood at 37°C (Winslow et al., 1977) are also shown in Table 4. The relatively large value that we find for n_{max}, in both the fresh and 2,3-DPG-depleted cases, indicates a high degree of cooperativity for the binding of O_2 to Hb A. It is difficult to conclude from our data whether n_{max} is higher or lower in the case of fresh samples or 2,3-DPG-depleted samples. In Hb A in solution, 2,3-DPG is thought to

strengthen the cooperativity (Antonini and Brunori, 1971; Imai, 1982). It is possible that other effectors present in the 2,3-DPG-depleted samples also affect the cooperativity of the oxygenation. As previously noted (Winslow et al., 1977; Imai, 1982), quantitative analysis of data in whole blood samples should be made with caution, because there is considerable variability among individuals.

From Figs. 6 and 7, we observe that there is a significant difference of perhaps as much as 10% in the preferential binding of oxygen to the α-chain versus the β-chain, as measured by the proximal histidyl resonances of deoxy-Hb A in fresh and 2,3-DPG-depleted erythrocytes. It is difficult to draw quantitative conclusions about the relative contributions of the effectors in this situation. Previous NMR experiments on purified Hb A (using the ferrous hyperfine-shifted proton resonances that occur at 17 ppm from DSS for the α-chain and at 23 ppm for the β-chain) have shown that the α-chain has an oxygen affinity higher than that of the β-chain under a variety of experimental conditions (Lindstrom and Ho, 1972; Johnson and Ho, 1974; Viggiano and Ho, 1979; Viggiano et al., 1979; Ho et al., 1982). The extent of the nonequivalence between the α- and β-chains for oxygen was found to depend on the nature and concentration of various allosteric effectors. Our present experiments on fresh erythrocytes were performed under nonsaturating conditions, with a molar ratio of 2,3-DPG to Hb A of $\sim$0.7. Thus, our present results on the nonequivalence between the α- and β-chains of Hb A with respect to oxygen binding in erythrocytes are in agreement with our early conclusions on the functional nonequivalence between the α- and β-chains of purified Hb A for oxygen in solution. For a review of the details of this subject, see Ho (1992).

Comparison of total Hb A saturation measurements

From comparison of the Hb A oxygen saturation, as measured by various methods (Fig. 8), it appears that the saturation Y_{AB} is a good indicator of the Hb A oxygen saturation in the sense that it agrees more closely with spectrophotometric measurements, whereas the saturation R is not a reliable indicator. The saturation R is smaller by up to about 15% of full saturation relative to both the spectrophotometric measurements and the measurements of the hyperfine-shifted, exchangeable $N_\delta H$ resonances of the proximal histidines of deoxy-Hb A, reaching a maximum deviation in the region $pO_2 \sim >70$ mmHg. The sum of the normalized areas of the resonances of deoxy-Hb A and HbO_2 A appears to be less than 100% for some regions of the oxygenation curve, reaching only about 85 to 90%. This value is about the same in both fresh and 2,3-DPG-depleted samples and occurs at about the same hemoglobin oxygen saturation levels, although not at the same pO_2.

There are several possible explanations for the difference in the oxygen saturation measurements. First, as previously discussed, the area of the oxy marker resonance may not be accurately quantified, because of errors in baseline estimation and overlapping resonances. However, the maximum difference occurs in a region where the HbO_2 A marker resonance is strong, so that interference from neighboring deoxy-Hb A resonances is not likely, although it cannot be completely ruled out. Second, it is possible that the T_1 and T_2 values of the oxy marker resonances may vary with percent oxygenation, because of the chemical exchange of magnetization between the unligated and oxygenated forms of hemoglobin, so that the relative weighting of the resonances due to T_1 and T_2 effects may vary with oxygenation. In the unligated form, the γ_2-CH_3 protons of the distal valine of the α- and β-chains of hemoglobin may be relaxed by the paramagnetic heme iron atoms. The linewidths of the marker resonances do not appear to change with percent oxygenation, so that the T_2 values are roughly constant and the resonances are not exchange-broadened. However, the T_1 values of these resonances in each sample are not known, so we cannot exclude this possibility. Both ^{1}H-NMR experiments using SUPERB pulse sequences were performed with a repetition time of about twice the T_1 relaxation time of their respective target resonances. Third, there may be effects due to differences in the cellular environment that decrease the signal from deoxy-Hb A and HbO_2 A differentially, such as magnetic susceptibility gradients (Fabry and San George, 1983). Tests of the marker resonances were run on fully oxygenated and deoxygenated packed erythrocytes, with the plasma removed from the top of the NMR tube. The cells were then lysed by a freeze-thaw method, and no significant decrease in the signal intensity was observed. This is expected, because the erythrocytes were packed. There may be differences between measurements on packed cells, on which NMR experiments were conducted, and on measurements on whole blood, on which blood-gas and spectrophotometric analysis was conducted. However, good agreement was obtained between the oxygen saturation as measured by the decrease in the deoxy marker resonances and by spectrophotometric analysis, so this possibility seems unlikely. Fourth, the deoxy-Hb A marker resonances originate from the $N_\delta H$ protons of the proximal histidyl side chain and are sensitive to the paramagnetic state of the heme iron and, thus, are directly correlated with the binding of oxygen. The HbO_2 A marker resonance, on the other hand, originates from the γ_2-CH_3 protons of the distal valine side chain and is sensitive to the conformation of the heme pocket, which does not necessarily correlate directly with the binding of oxygen. The HbO_2 A marker resonance appears to correlate with a change in the conformation of the heme pocket that occurs after the oxygen is bound. However, there are many other factors that may influence the conformation of the heme pocket, including a variety of oxygen-binding effectors, and no definitive conclusion may be drawn at the present.

It is also possible that the distal valine resonance correlates with a tertiary and/or quaternary structural change of Hb A, based on the number of subunits ligated. A comparison of the populations of partially ligated species of Hb A, calculated based on the saturation of Hb A measured from the deoxy-Hb

A resonances, Y_{AB}, with the area of the HbO_2 A marker resonance, R, is shown in Fig. 9. The binding constants of the sequential tetrahedral binding model (Koshland et al., 1966) were used to calculate the number of partially ligated subunits (for details, see Fetler, 1993). Given the accuracy of the data, the subunit populations shown in Fig. 9 should be treated only as a rough, qualitative indication of the population trends. It appears that the area of the HbO_2 A marker resonance is less than the number of ligated subunits and correlates most closely with the number of fully oxygenated tetramers, $Hb[O_2]_4$. Further work is needed to understand our observations.

The conditions of our experiments (Table 2) are not quite the same as the average physiological conditions (Woodson et al., 1970; Winslow et al., 1977). Nevertheless, our results give an indication of the general trends to expect in vivo. One potential complication of using these methods in vivo is the interference from overlapping resonances of deoxy-Mb and MbO_2 in similar positions (Wang et al., 1990; Jue and Anderson, 1990; Kreutzer and Jue, 1991; Kreutzer et al., 1992). However, with the SUPERB selective excitation method, which eliminates the phase gradient in the spectra, we should be able to estimate accurately the contributions of these resonances. This may be difficult to do using other methods, such as those previously used to measure deoxy-Mb and MbO_2 in vivo (Wang et al., 1990; Jue and Anderson, 1990; Kreutzer and Jue, 1991; Kreutzer et al., 1992). These types of measurements may be used, perhaps, to supplement the information obtained from functional imaging studies (Kwong et al., 1992), which are based on the paramagnetic effect of deoxy-Hb A.

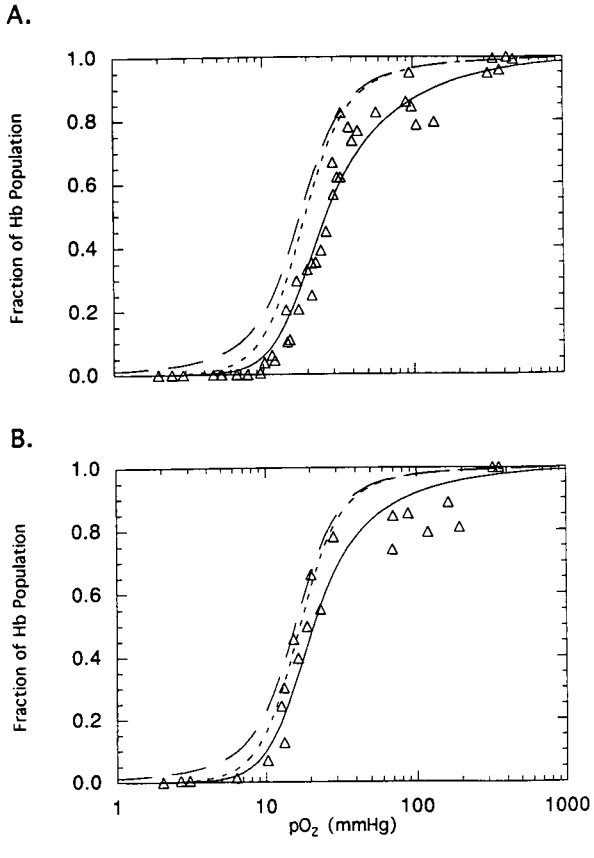

FIGURE 9 Comparison of fractional area R of HbO_2 A marker resonance (△), with the number of ligated subunits (– – –), the contribution of triply- and quadruply ligated tetramers, 0.75 $Hb(O_2)_3$ + $Hb(O_2)_4$ (- - - -), and the number of fully ligated tetramers, $Hb(O_2)_4$ (——): (*A*) fresh erythrocytes; (*B*) 2,3-DPG-depleted erythrocytes.

CONCLUSION

We are able to measure the percent oxygenation of the α- and β-chains of Hb A inside packed erythrocytes with improved ¹H-NMR methods, using resonances of both deoxy-Hb A and HbO_2 A. We have found that the hyperfine-shifted, exchangeable $N_\delta H$ proton resonances of the proximal histidines of the α- and β-chains of deoxy-Hb A correlate well with the binding of oxygen to the hemes. From these resonances, we have also found that there is a preference for oxygen to bind to the α-chain (up to 10%) over the β-chain of Hb A, in both the absence of 2,3-DPG and in equimolar 2,3-DPG. The present measurements concur with our previous results obtained on purified Hb A samples, within the margins of error. On the other hand, we find that the γ_2-CH_3 proton resonances of the distal valines of HbO_2 A are sensitive to a change in conformation of the heme pocket, which is not directly correlated with the oxygen saturation, and most likely occurs after the binding of oxygen to the heme iron atoms.

Improvements in our ¹H-NMR selective excitation method, SUPERB (Fetler et al., 1993), lead to wide-band uniform phase excitation and pulse shape-insensitive suppression of the water signal. The improvements enhance the degree of water suppression routinely obtainable by an order of magnitude and allow for quantitative measurement of the signals of interest in the presence of overlapping signals. This method should be useful for a wide variety of applications in ¹H-NMR spectroscopy.

We thank Mark R. Busch, Patricia F. Cottam, Susan R. Dowd, Nancy T. Ho, and Michael C. Schrader for their expert advice and assistance with sample preparation. We are grateful to the Central Blood Bank of Pittsburgh for providing blood samples needed for our work.
This work was supported by National Institutes of Health grants RR-03631 and HL-24525.

APPENDIX

We summarize the theory of *S*mall flip-angle pulse sequences with a simultaneous *U*niform *P*hase *E*xcitation *R*egion and *B*inomial-type null, or SUPERB (Fetler et al., 1993), as follows: for a sequence of N_f hard pulses applied along the $-y$ axis and evenly separated by an interpulse delay τ, with initial magnetization along the $+z$ axis, the transverse magnetization $M_+ = M_x + iM_y$ may be written

$$M_+(\Delta\omega) \approx \sum_{n=0}^{N_f-1} \theta_{tot} f_n \exp[i(n + x)\Delta\omega\tau], \quad (3)$$

where $\Delta\omega$ is the offset frequency from the carrier, θ_{tot} is the total flip angle at $\Delta\omega = \pi/\tau$, f_n is the flip angle of the nth pulse as a fraction of θ_{tot}, and x is the ratio of t_{DE} to τ, where t_{DE} is a delay added to the end of the pulse sequence, such that $x = t_{DE}/\tau$. The rotation angle for a spin off-resonance

by $\Delta\omega$ during the delay τ is $\Delta\omega\tau$. For the case $x = 0$, c_m, the mth-order derivative of M_+ at an arbitrary offset frequency ω_c, is

$$c_m = \theta_{tot} \sum_{n=0}^{N_f-1} f_n (in\tau)^m \exp(in\omega_c\tau). \quad (4)$$

This method is, of course, a generalization of the method used to derive the binomial pulse sequences (Hore, 1983). We select a set of derivatives $\{c_m\}$ for each offset frequency ω_c, and solve the set of equations $\{c_m\} = \{d_m\}$, where d_m is the mth desired value for c_m, for the relative pulse lengths $\{f_n\}$. Previously, for the SUPERB-O and SUPERB-A pulse sequences (Fetler et al., 1993), we chose $d_m = 0$ only for $\omega_c = 0$ and $\omega_c = \pi/\tau$. As we increase the order of the odd vanishing derivatives for $\omega_c = \pi/\tau$, it is increasingly difficult to widen the bandwidth of the uniform phase excitation region. This method produces coefficients in Eq. 4 of up to the order of $(N_f)^{M_m}$, where M_m is the order of the highest-order derivative. The ratio of the maximum pulse length to minimum pulse length is about the same order of magnitude. This may formally be shown, for example, by use of Cramer's Rule for solution of linear systems (Burden and Faires, 1985). Thus, the pulse sequences become increasingly difficult to implement experimentally. However, we may achieve a wider bandwidth of uniform phase excitation, although with some "ripple" effects, using the following set of equations

$$c_m = 0 = \theta_{tot} \sum_n f_n n^m; \qquad \omega_c = 0; \qquad m = 0 \text{ to } M_a; \quad (5)$$

$$cy_0 = 0 = \theta_{tot} \sum_n f_n \sin(n\omega_c\tau); \qquad \omega_c = \frac{k\pi}{\tau N_f};$$
$$k = (M_a + 2) \text{ to } (N_f - 1), \quad (6)$$

where cy_0 is the imaginary part of c_0. We also add the normalization condition $cx_0 = 1$ for $\omega_c = \pi/\tau$. As with the SUPERB-O and SUPERB-A pulse sequences, Eqs. 5 and 6, plus the normalization condition, form a set of N_f linearly independent equations in the N_f flip angles $\{f_n\}$, which we may easily solve. Eq. 6 produces pure real phase at the offset frequencies specified because cx_0, the real part of c_0, generally does not vanish. Note that $cy_0 = 0$ is implicitly true for $\omega_c = \pi/\tau$. We refer to these pulse sequences by the acronym SUPERB-W(M_a, $[M_a + 2]\pi/N_f$), where "W" stands for *W*ide bandwidth uniform phase excitation, M_a is the order of the highest-order vanishing derivative of the magnetization at $\Delta\omega = 0$, and $(M_a + 2)\pi/N_f$ is the edge of the uniform phase excitation region times the interpulse delay τ. The bandwidth of the uniform phase excitation region is $2[N_f - (M_a + 2)]\pi/(\tau N_f)$, which is centered about $\Delta\omega = \pi/\tau$. In addition, the ratio of the coefficients, and therefore the ratio of maximum to minimum pulse lengths, is of the order $[(N_f)^{M_a}]/[\sin(\pi/N_f)]$, which is usually a smaller number than $[(N_f)^{M_m}$, so these pulse sequences are more easily produced experimentally than SUPERB-O or -A. Equations 5 and 6 seem to be the limit of uniform phase excitation producible; if we choose the slightly more spread out values of $\omega_c = k\pi/[\tau(N_f - 1)]$ for $k = (M_a + 1)$ to $(N_f - 2)$ in Eq. 6, we obtain a linear phase roll that passes through zero at these values of ω_c.

If we choose $x \neq 0$, new solutions may be found by modifying Eq. 6 such that

$$\omega_c = [(k + x)\pi]/[\tau(N_f + x)]. \quad (7)$$

Thus, the distribution of frequencies for optimized phase is slightly narrower. The best solutions are found for $x = 0.5$, because the excitation regions on either side of the null then have exactly 180° phase difference.

REFERENCES

Antonini, E., and M. Brunori. 1971. Hemoglobin and Myoglobin in Their Reactions With Ligands. North-Holland, Amsterdam.

Benesch, R., and R. E. Benesch. 1967. The effect of organic phosphates from human erythrocyte on the allosteric properties of hemoglobin. *Biochem. Biophys. Res. Commun.* 26:162–167.

Bevington, P. R., and D. K. Robinson. 1992. Data Reduction and Error Analysis for the Physical Sciences. McGraw-Hill, New York.

Bunn, H. F., B. J. Ransil, and A. Chao. 1971. The interaction between erythrocyte organic phosphates, magnesium ion, and hemoglobin. *J. Biol. Chem.* 246:5273–5279.

Burden, R. L., and J. D. Faires. 1985. Numerical Analysis. Prindle, Weber, and Schmidt, Boston, MA.

Carr, H. Y., and E. M. Purcell. 1954. Effects of diffusion on free precession in nuclear magnetic resonance experiments. *Phys. Rev.* 94:630–638.

Chanutin, A., and R. R. Curnish. Effect of organic, and inorganic phosphates on the oxygen equilibrium of human erythrocytes. *Arch. Biochem. Biophys.* 121:96–102.

Craescu, C. T., C. Poyart, C. Scharffer, M.-C. Garel, J. Kister, and Y. Beuzard. 1986. Covalent binding of glutathione to hemoglobin. II. Functional consequences and structural changes reflected in NMR spectra. *J. Biol. Chem.* 261:14710–14716.

Dalvit, C., and C. Ho. 1985. Proton nuclear Overhauser effect investigation of the heme pockets in ligated hemoglobin: conformational differences between oxy and carbonmonoxy forms. *Biochemistry.* 24: 3398–3407.

Dickerson, R. E., and I. Geis. 1983. Hemoglobin: Structure, Function, Evolution, and Pathology. Benjamin-Cummings, Menlo Park, CA.

Englander, S. W., D. B. Calhoun, and J. J. Englander. 1987. Biochemistry without Oxygen. *Anal. Biochem.* 161:300–306.

Fabry, M. E., and R. C. San George. 1983. Effect of magnetic susceptibility on nuclear magnetic resonance signals arising from red cells: a warning. *Biochemistry.* 22:4119–4125.

Fetler, B. K. 1993. Development of selective excitation methods in NMR: investigation of hemoglobin oxygenation in erythrocytes using ^{1}H- and ^{31}P-NMR. Ph.D. thesis. Department of Physics, Carnegie Mellon University, Pittsburgh, PA.

Fetler, B. K., V. Simplaceanu, N. S. VanderVen, I. J. Lowe, and C. Ho. 1993. Design of pulse sequences for solvent suppression and uniform excitation. Application to observing hemoglobin in solution and inside red blood cells. *J. Magn. Reson. Ser. B.* 101:17–27.

Gasparovic, C., and N. A. Matwiyoff. 1992. The Magnetic properties and water dynamics of the red blood cell: a study by proton NMR lineshape analysis. *Magn. Reson. Med.* 26:274–299.

Gupta, R. K., J. L. Benovic, and Z. B. Rose. 1978. Magnetic resonances studies of the binding of ATP and cations to human hemoglobin. *J. Biol. Chem.* 253:6165–6171.

Hamasaki, N., and Z. B. Rose. 1974. The binding of phosphorylated red cell metabolites to human hemoglobin A. *J. Biol. Chem.* 253:7896–7901.

Ho, C. 1992. Proton nuclear magnetic resonance studies on hemoglobin: cooperative interactions and partially ligated intermediates. *Adv. Prot. Chem.* 43:153–312.

Ho, C., C.-H. J. Lam, S. Takahashi, and G. Viggiano. 1982. ^{1}H-NMR studies of cooperative oxygenation of normal human adult hemoglobin. *In* Hemoglobin and Oxygen Binding. C. Ho, editor. Elsevier North Holland, Amsterdam. 141–149.

Hore, P. J. Solvent suppression in Fourier transform nuclear magnetic resonance. *J. Magn. Reson.* 55:283–300.

Hoult, D. I. 1979. The solution of the Bloch equations in the presence of a varying B_1 field—an approach to selective pulse analysis. *J. Magn. Reson.* 35:69–86.

Imai, K. 1982. Allosteric Effects in Haemoglobin. Cambridge University Press, Cambridge.

Johnson, M. E., and C. Ho. 1974. Effects of ligands and organic phosphates on functional properties of human adult hemoglobin. *Biochemistry.* 13: 3653–3661.

Jue, T., and S. Anderson. 1990. ^{1}H Observation of tissue myoglobin: an indicator of intracellular oxygenation in vivo. *Magn. Reson. Med.* 13: 524–528.

Kirk, K., and P. W. Kuchel. 1988. The contribution of magnetic susceptibility effects to transmembrane chemical shift differences in the ^{31}P NMR spectra of oxygenated erythrocyte suspensions. *J. Biol. Chem.* 263: 130–134.

Koshland, D. E., G. Némethy, and D. Filmer. 1966. Comparison of experimental binding data and theoretical models in proteins containing subunits. *Biochemistry.* 5:365–385.

Kreutzer, U., and T. Jue. 1991. ^{1}H-Nuclear magnetic resonance deoxymyoglobin signal as indicator of intracellular oxygenation in myocardium. *Am. J. Physiol.* 261:H2091–H2097.

Kreutzer, U., D. S. Wang, and T. Jue. 1992. Observing the ^{1}H NMR signal of the myoglobin Val-E11 in myocardium: an index of cellular oxygenation. *Proc. Natl. Acad. Sci. USA.* 89:4731–4733.

Kwong, K. K., J. W. Belliveau, D. A. Chesler, I. E. Goldberg, R. M. Weisskopf, B. P. Poncelet, D. N. Kennedy, B. E. Hoppel, M. S. Cohen, R. Turner, H.-M. Cheng, T. J. Brady, and B. R. Rosen. 1992. Dynamic magnetic resonance imaging of human brain activity during primary sensory stimulation. *Proc. Natl. Acad. Sci. USA.* 89: 5675–5679.

Labotka, R. J. 1984. Measurement of intracellular pH and deoxyhemoglobin concentration in deoxygenated erythrocytes by phosphorus-31 nuclear magnetic resonance. *Biochemistry.* 23:5549–5555.

Lam, Y.-F., A. K.-L. C. Lin, and C. Ho. 1979. A phosphorus-31 nuclear magnetic resonance investigation of intracellular environment in human normal and sickle cell blood. *Blood.* 54:196–209.

La Mar, G. N., K. Nagai, T. Jue, D. L. Budd, K. Gersonde, H. Sick, T. Kagimoto, A. Hayashi, and F. Taketa. 1980. Assignment of proximal histidyl imidazole exchangeable proton NMR resonances to individual subunits in hemoglobins A, Boston, Iwate, and Milwaukee. *Biochem. Biophys. Res. Commun.* 96:1172–1177.

Lindstrom, T. R., and C. Ho. 1972. Functional nonequivalence of α and β hemes in human adult hemoglobin. *Proc. Natl. Acad. Sci. USA.* 69:1707–1710.

Lindstrom, T. R., and C. Ho. 1973. Effects of anions and ligands on the tertiary structure around ligand binding site in human adult hemoglobin. *Biochemistry* 12:134–139.

Lindstrom, T. R., I. B. E. Norén, S. Charache, H. Lehmann, and C. Ho. 1972. Nuclear magnetic resonance studies of hemoglobins. VII. tertiary structure around ligand binding site in carbonmonoxyhemoglobin. *Biochemistry* 11:1677–1681.

Meiboom, S., and D. Gill. 1958. Modified spin-echo method for measuring nuclear relaxation times. *Rev. Sci. Instr.* 29:688–691.

Morris, G. A., and R. Freeman. 1978. Selective excitation in fourier transform nuclear magnetic resonance. *J. Magn. Reson.* 29:433–462.

Press, W. H., B. P. Flannery, S. A. Teukolsky, and W. H. Vetterling. 1986. Numerical Recipes. Cambridge University Press, Cambridge.

Sachs, J. R., P. A. Knauf, and P. B. Dunham. 1975. Transport through red cell membranes. *In* The Red Blood Cell. D. M. Surgenor, editor. Academic Press, New York. 613–705.

Starčuk, Z., and V. Sklenář. 1985. New hard pulse sequences for the solvent signal suppression in fourier-transform NMR. *J. Magn. Reson.* 61:567–570.

Takahashi, S., A. K.-L. C. Lin, and C. Ho. 1980. Proton nuclear magnetic resonance studies of hemoglobins M Boston (α58E7 His $\rightarrow$ Tyr) and M Milwaukee (β67E11 Val $\rightarrow$ Glu): spectral assignments of hyperfine-shifted proton resonances and of proximal histidine (E7) NH resonances to the α and β chains of normal human adult hemoglobin. *Biochemistry.* 19:5196–5202.

Tehrani, A. Y., Y.-F. Lam, A. K.-L. C. Lin, S. F. Dosch, and C. Ho. 1982. Phosphorus-31 nuclear magnetic resonance studies of human red blood cells. *Blood Cells.* 8:245–261.

Tyuma, I., K. Imai, and K. Shimizu. 1973. Analysis of oxygen equilibrium of hemoglobin and control mechanism of organic phosphates. *Biochemistry.* 12:1491–1498.

Viggiano, G., and C. Ho. 1979. Proton Nuclear Magnetic Resonance Investigation of Structural Changes Associated with Cooperative Oxygenation of Human adult hemoglobin. *Proc. Natl. Acad. Sci. USA.* 76:3673–3677.

Viggiano, G., N. T. Ho, and C. Ho. 1979. Proton nuclear magnetic resonance and biochemical studies of oxygenation of human adult hemoglobin in deuterium oxide. *Biochemistry.* 18:5238–5247.

Wang, Z., E. A. Noyszewski, and J. S. Leigh, Jr. 1990. In vivo MRS measurement of deoxyhemoglobin in human forearm. *Magn. Reson. Med.* 14:562–567.

Winslow, R. M., M.-L. Swenberg, R. L. Berger, R. I. Shrager, M. Luzzana, M. Samaja, and L. Rossi-Bernardi. 1977. Oxygen equilibrium curve of normal human blood and its evaluation by Adair's equation. *J. Biol. Chem.* 252:2331–2337.

Wodak, S. J., J.-L. D. Coen, S. J. Edelstein, H. Demarne, and Y. Beuzard. 1986. Modification of human hemoglobin by glutathione. III. Perturbations of hemoglobin conformation analyzed by computer modeling. *J. Biol. Chem.* 261:14717–14724.

Woodson, R. D., J. D. Torrance, D. S. Shappell, C. Lenfant. 1970. The effect of cardiac disease on hemoglobin-oxygen binding. *J. Clin. Invest.* 49: 1349–1356.

Yao, C., V. Simplaceanu, A. K.-L. C. Lin, and C. Ho. 1986. Bloch analysis and solvent suppression by soft pulses. Application to proton NMR investigations of human hemoglobin in H_2O in intact red blood cells. *J. Magn. Reson.* 66:43–57.